

# EFFECT OF COLUMN DIAMETER ON PRESSURE DROP OF A CORRUGATED SHEET STRUCTURED PACKING

Ž. OLUJIC

*Laboratory for Process Equipment, Delft University of Technology, The Netherlands*

The results of an experimental study indicating a significant effect of column diameter on the pressure drop and capacity of corrugated sheet structured packing are presented. The experiments were carried out with Montz-pak B1-250, using an air/water system at ambient conditions in perspex columns with internal diameters of 0.2 m, 0.45 m, 0.8 m and 1.4 m. The results clearly show that both the pressure drop increase and capacity decrease become significant when the column diameter approaches the value equal to that of the height of a packing element. This observation suggests that column diameter(s) based on small scale data can be too large.

*Keywords: structured packing; pressure drop; diameter effect; scale-up*

## INTRODUCTION

Corrugated sheet structured packing is now a well established gas/liquid contacting device not only in distillation but also in many related heat and mass transfer applications. Owing to its often superior capacity/efficiency characteristics, it is nowadays considered as first choice, and many column designers in their capacity/diameter considerations rely on performance prediction methods available in commercial software packages.

Although a considerable experimental effort has been undertaken to substitute development of empirically based performance models, an important scale-up aspect, i.e. relationship between column diameter and the performance of structured packing, has not received enough attention in the open literature. From a very limited number of observations<sup>1-3</sup> summarized in the book by Kister<sup>4</sup>, it appeared that the pressure drop of structured packing tends to decrease with the increase in the column diameter, which is a reverse effect with respect to that observed with random packings. A simple but correct explanation for such behaviour of structured packings can be found in a recent paper by Brunazzi and Paglianti<sup>5</sup>, namely in a relatively larger number of bends in gas flow in small diameter columns. Anyhow, nothing is publicly known about the magnitude of the column diameter effect.

Certainly, pressure drop is a major design parameter influencing directly the capacity/diameter of distillation and related gas-liquid contacting columns. Therefore, it is highly desirable for designers of packed columns to have at their disposal a reliable pressure drop estimation method. It is generally unreasonable to expect that reliable pressure drop prediction methods may be developed from experimental work on structured packings in small diameter columns. In other words, the badly needed information is that coming from an experiment carried out at a scale large enough to represent industrial situations. Packing manufacturers and some users are aware of this; however, their large-scale data are not publicly available. In the early days,

Sulzer published some data on pressure drop of Mellapak 250 Y suggesting a considerable diameter effect<sup>2</sup>. The air/water data on the pressure drop of Mellapak 250 in a 0.3 and a 1 m diameter column can also be found in a recent paper by Olujić and de Graauw<sup>6</sup>. This reference also shows a comparison of own air/water data obtained with Montz-pak B1-250 in columns with internal diameters (ID) of 0.45 m and 0.8 m, indicating a more pronounced liquid load effect in smaller diameter column.

In order to get some certainty with respect to the lower and upper diameter limits, the experimental base was extended by including the results obtained most recently using a 0.192 m and a 1.4 m ID perspex column. The purpose of this communication is to describe the large-scale experiment and to compare the results with those obtained with the same packing in columns with smaller diameters. In this way, experimental evidence was obtained that gives a fair indication of the nature and the size of the expected column diameter effect.

## EXPERIMENTAL

The experiments summarized in this paper have been carried out with a common size, conventional type corrugated sheet structured packing using similar test installations available at TU Delft and J. Montz in Hilden, Germany. The experimental rig of TU Delft includes two separate installations, one for small- and another one for large scale hydraulic experiments, with 0.45 m and 1.4 m ID columns made of perspex/plexiglass. An additional 0.192 m ID perspex column was placed in a small scale installation, using a uniformly converging diameter reduction piece. The multifunctional column hydraulics installation available in Hilden contains a 0.8 m ID perspex column. In all cases, the test system was air/water, at atmospheric pressure and ambient temperature, and the packing used was Montz-pak B1-250. This packing is made of unperforated, sheet metal with a shallow embossed surface with

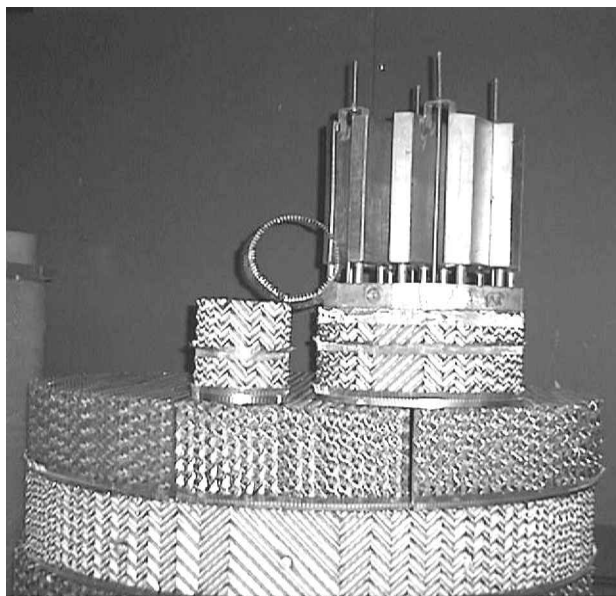


Figure 1. Photograph showing Montz-pak B1-250 elements with different diameters, a narrow trough distributor and a wall wiper ring as employed in this study.

corrugations inclined at an angle of 45 degrees. Figure 1 shows a photograph of packing elements used in the experiments carried out in Delft. In all cases the packing was equipped with a strong liquid scraper ring (wall wiper) placed at the bottom of each packing element, with a saw-tooth-like bottom part bent inwards. The liquid distributors were all of the narrow trough type with drip tubes (see Figure 1), with orifices in the tube side. The initial distribution point (tube) density in columns with 0.45 and 0.8 m was 100 and in the 1.4 m diameter column 145 drip points per  $\text{m}^2$ . In the case of the 0.192 m ID column, a section containing 4 tubes of the narrow trough distributor was used, which corresponds roughly to 200 d.p./ $\text{m}^2$ . The outlets of the drip tubes were in each case placed approximately 20 mm above the packing, and the distributor rotated with respect to the orientation of the top layer of the packing to ensure that liquid is distributed over the largest possible number of channels formed between corrugated sheets.

Three independent, but essentially equal test installations were used. The largest one, is described here, namely the TU industrial scale column hydraulics' simulator, with a 1.4 m ID column assembled of flanged perspex sections with a total height of 6 m. As shown schematically in Figure 2, the gas inlet is placed centrally in the bottom/sump part of the column made of SS, ending with a 'Chinese hat' cover. This kind of initial gas distribution was chosen because of its simplicity and minimum space requirement. The gas distributors in smaller diameter columns were common side inlets, a half-open tube in Delft and a perforated (sparger) tube in Hilden. Packing was placed on an elevated support to enable visual contact with the bottom of the installed bed. As indicated in Figure 2, water followed a closed circuit. It was drawn from a 5  $\text{m}^3$  liquid tank and pumped through the pipes with flowmeters up to the distributor, from which it flowed over the packing and via the column sump, back into the supply tank. Liquid was distributed over the packing using a large turnaround, Montz-type narrow trough distributor with 145 d.p./ $\text{m}^2$ . Air was taken from the surroundings and supplied to the column from a blower and metered by an

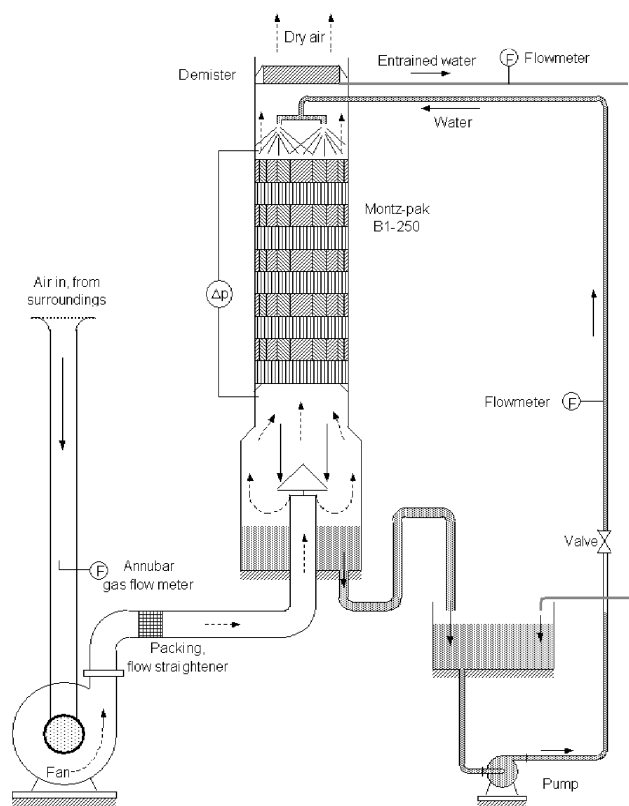


Figure 2. Schematic of the TU Delft packed column hydraulics' simulator ( $d = 1.4$  m,  $h = 6$  m).

Annubar flowmeter, i.e. a multiple pitot tube device placed in the 7 m tall 0.6 m ID gas intake tube. To comply fully with requirements for a developed air flow profile under all operating conditions, the flow meters are placed 5 m from the rounded inlet of the air supply tube. An element of Montz-pak B1-250 was installed downstream of the blower to act as a flow straightener as well as a vortex-breaker in the vertical section immediately below the 'Chinese hat'. A number of calibration experiments were carried out to get certainty about the accuracy of the measurement of air-flow rate, and it was estimated that it was within 5%. The powerful (130 kW) blower was equipped with an electronic device for control of the number of rotor revolutions, which contributed to a very smooth operation, and most importantly reduced significantly the noise associated with full power operation.

In order to avoid possible relative deviations in measured air flow rates between test units, a standard pitot tube was used in all cases to calibrate the installed flow meters.

Pressure drop gradient over the bed was measured using a U-tube manometer filled with water. Each test began by pumping the liquid over the packing at a high liquid flow rate to ensure thorough wetting of the packing. The liquid flow was then stopped for a while to allow excessive liquid to drain from the packing. After setting the desired liquid load, the gas flow rate was increased in steps up to the flooding condition, while readings were taken of air flow, water flow, pressure drop, water temperature and column inlet and outlet gas temperatures. Surrounding air temperature and humidity were recorded before and after each of test series. Visual observations were made and noted accordingly. The onset of loading manifested itself as liquid build up at wall wiper rings, starting usually at the lowest packing element.

## RESULTS AND DISCUSSION

The experimental results for dry packing are summarized in the log-log graph shown in Figure 3, where measured values of the overall pressure drop are plotted against the gas load factor ( $F$ -factor =  $F_G = u_{Gs} \sqrt{\rho_G}$ ) with column diameter as a parameter. The measured points exhibit the expected straight-line trend, indicating a pronounced increase in pressure drop with decreasing diameter, with a relatively small difference between 0.45, 0.8 and 1.4 m ID columns. An additional series of results, measured in the column with the smallest diameter indicates a rather strong effect of the wall wiper, which is not strange if one considers the design employed in this study. Namely, with the saw-tooth-like section bent inward the effective cross sectional area for gas flow is reduced by nearly 10%. This is substantial, and in irrigated packing leads also to a considerable decrease in capacity. This can be conjectured from Figure 4, which is a typical plot of pressure drop measured in wet conditions. Here each measured series exhibits a change in the slope of the curve. This can be roughly approximated by two straight lines with the intersection indicating the loading point gas load, i.e. the point of the onset of a progressive liquid build-up, accompanied by a correspondingly sharp rise in pressure drop with increasing gas load. As is well known, above the loading point the upwardly flowing gas hinders the downward flow of the liquid and liquid starts to accumulate at the transitions between packing elements (layers). Generally, with increasing liquid load the loading point will shift to lower gas load, and, as shown in Figure 4, the same seems to occur with decreasing column diameter.

This observation may have serious practical implications because it suggests that at the same gas load there is a much lower pressure drop, and at the same pressure drop considerably larger capacity can be expected in a large diameter column. This means that pressure drop predictions based on small column diameter data can result in column diameters, larger than those associated with even the most conservative designs.

In a small diameter column, the increased dry pressure drop may be attributed mainly to a relatively larger number of sharp changes in gas flow direction per element height and this effect becomes stronger in the presence of liquid. Namely, a direction change on the wall is enforced by wall wipers, which, loaded with liquid create an impenetrable obstacle for gas flow. Since liquid is reflected from the walls, an overload of liquid is created in the wall zone, which forces the larger part of the gas flow to avoid the

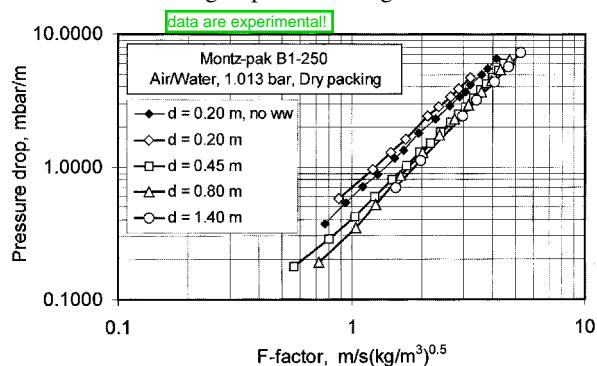


Figure 3. Influence of column diameter on dry pressure drop of Montz-pak B1-250, with indication of wall wiper effect.

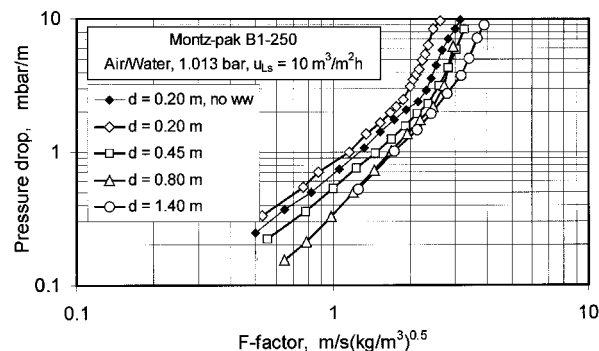


Figure 4. Influence of column diameter on wet pressure drop of Montz-pak B1-250, with indication of wall wiper effect.

wall, i.e. to make a sharp bend within the packing element and escape toward the bulk of the packing using channels less loaded by liquid than those in the wall zone. Indeed our liquid distribution experiments carried out in a column with 0.5 m ID have indicated that the wall zone, unable to get rid of the liquid transported to the walls, tends to operate overloaded by liquid, and this is pronounced to an extent depending on the spreading characteristics of the packing and liquid properties. A more or less pronounced segregation of liquid load occurred in the loading region with all packings tested<sup>7</sup>. In larger diameter columns, there is no additional resistance from the bulk side and gas spreads throughout the packing element at the expense of a slightly increased pressure drop, needed to equalize the static pressure in each cross section along the column. On the other hand, in a column with a diameter equal to a doubled packing element height or smaller, the liquid overload in the wall zone reduces the available cross section area significantly, forcing gas to flow at an average velocity substantially higher than that experienced at the same gas load in a column with a larger diameter, making at the same time (additional) sharp bends within each packing element height.

Summing up, it appears that the observed column diameter effect is strongly related to the number of sharp direction changes experienced by gas ascending through a packing element, as well as to the extent of the reduction in column cross sectional area due to wall wipers and liquid overload of the packing periphery. This suggests that the hydraulic operation of a packed bed consisting of corrugated sheet structured packing can be divided into two characteristic zones, the wall zone and the bulk zone, implying that a column with a diameter equal or lower than the packing height operates in wall-zone mode.

## MODEL VALIDATION

According to the Delft Overall Performance Model<sup>8</sup> the static pressure gradient of a bed assembled of corrugated sheet structured packing consists of three distinct contributions:

$$\begin{aligned} \Delta p &= \Delta p_{GL} + \Delta p_{GG} + \Delta p_{DC} \\ &= F_{load} (\zeta_{GL} + \zeta_{GG} + \zeta_{DC}) \frac{\rho_G u_{Ge}^2}{2} \end{aligned} \quad (1)$$

where subscripts  $GL$ ,  $GG$  and  $DC$  respectively refer to pressure losses associated with the gas-liquid film surface interaction,

gas-gas interaction at the interface created between crossing gas flows, and direction changes at the transitions between packing elements and in the wall zone. In the right hand expression describing the overall pressure drop over the entire range of gas load,  $u_{Ge}$  is effective gas velocity, which is always greater than the superficial velocity,  $\rho_G$  is gas density, and  $F_{load}$  is a pressure drop enhancement factor in the loading region.  $\zeta_{GL}$ ,  $\zeta_{GG}$  and  $\zeta_{DC}$  represent corresponding flow resistance coefficients.

The first two, described in greater detail in the Appendix, are considered to be independent of the column diameter, and the latter one is involved with the observed effect. Although it is not justified theoretically to assume the pressure drop in the wall zone to be larger than that in the bulk of the packing, for practical reasons it was considered to consist of two resistances in series. The corresponding overall coefficient for direction change related losses is described as

$$\zeta_{DC} = \frac{h_{pb}}{h_{pe}} (\zeta_{bulk} + \psi \zeta_{wall}) \quad (2)$$

where  $h_{pb}$  is packed bed height,  $h_{pe}$  is packing element height, and  $\zeta_{bulk}$  and  $\zeta_{wall}$  are the characteristic form drag coefficients for bulk- and wall zone, respectively.  $\psi$  represents the ratio of the number of gas flow channels ending at column walls and the number of gas flow channels in the bottom cross section of a packing element or layer, i.e. the fraction of the total number of gas flow channels ending at column walls.

Figure 5 shows schematically a packing element, indicating channels ending at column walls. Obviously, the largest distance of the inlet of a channel ending at the wall, i.e. the width of the wall zone ( $m = h_{pe}/\tan \alpha$ ) depends on the height of the packing element and the corrugation inclination angle. The enclosed top view illustrates the distribution of channel inlets ending at column walls and the in top section of a packing element. In zone 1, both the channels oriented to the left- and the channels oriented to the right hand side reach the top cross section of a packing element. In zone 2, only the channels oriented to the left reach the top cross section of the packing element. The other half, i.e. the channels oriented to the right hand side, end on the column walls. All of the channels from zone 3 end on the column walls. The number of channels ending at the column walls corresponds with the sum of the cross sectional area of zone 3 and one half of the cross sectional area of zone 2. Dividing by the cross sectional area of the column and transforming into the corresponding geometric expressions yields the following definition for the fraction of gas flow channels ending at column walls

$$\psi = \frac{2h_{pe}}{\pi d_c^2 \tan \alpha} \left( d_c^2 - \frac{h_{pe}^2}{\tan^2 \alpha} \right)^{0.5} + \frac{2}{\pi} \arcsin \left( \frac{h_{pe}}{d_c \tan \alpha} \right) \quad (3)$$

where  $d_c$  is column diameter and  $\alpha$  is the corrugation inclination angle.

Figure 6 shows the fraction of the gas flow channels ending at column walls as a function of column diameter for two common corrugation inclination angles and three different packing element heights. In a column with a diameter of 1 m containing a 45° packing with element height of 0.2 m, approximately 25% of all gas flow channels

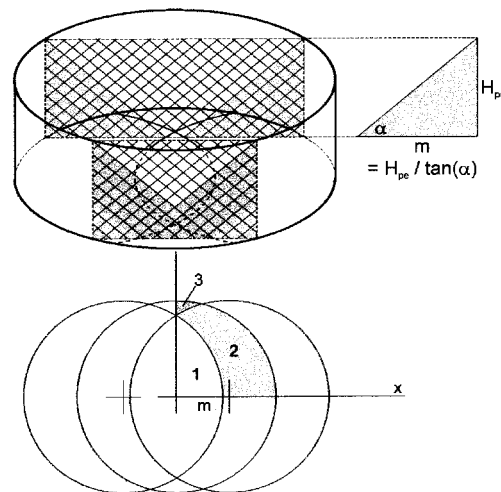


Figure 5. Drawing of a packing element illustrating the fraction of gas flow channels ending at column walls.

will end on column walls. Obviously, the pressure drop enhancement effect of the wall zone will weaken with increasing corrugation angle and decreasing element height, and consequently be less pronounced in common wire gauze- than sheet metal packings.

Because of a rather strong corrugation angle effect, the bulk zone direction change coefficient is expressed as a function of the corrugation angle alone.

$$\zeta_{bulk} = 1.76(\cos \alpha)^{1.63} \quad (4)$$

A more complex situation is in the wall zone, where an interaction of liquid and gas phases plays an important role, and is accounted for accordingly in the following empirical correlation.

$$\zeta_{wall} = \frac{4092 u_{Ls}^{0.31} + 4715 (\cos \alpha)^{0.445}}{Re_{Ge}} + 34.19 u_{Ls}^{0.44} (\cos \alpha)^{0.779} \quad (5)$$

where  $u_{Ls}$  is liquid superficial velocity.  $Re_{Ge}$  is a Reynolds number based on the effective gas velocity ( $u_{Ge}$ ):

$$Re_{Ge} = \frac{u_{Ge} \rho_G d_{hG}}{\mu_G} = \frac{u_{Gs}}{\sin \alpha (\epsilon - h_L)} \frac{\rho_G d_{hG}}{\mu_G} \quad (6)$$

where  $u_{Gs}$  is superficial gas velocity,  $\rho_G$  is gas density,  $\mu_G$  is gas dynamic viscosity,  $d_{hG}$  is hydraulic diameter of gas flow channel,  $\epsilon$  is packing porosity and  $h_L$  is liquid holdup.

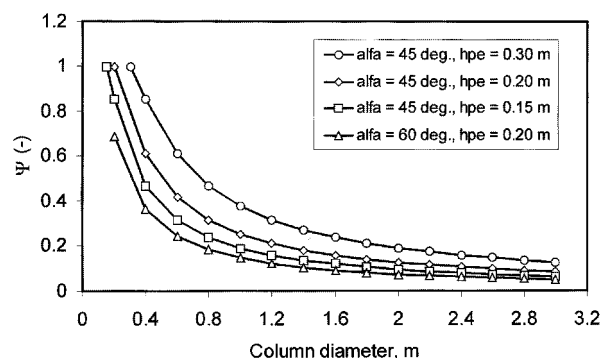


Figure 6. Fraction of the gas flow channels ending on the column walls as a function of corrugation angle and the packing element height.

Under the assumption of complete wetting, the liquid holdup follows simply from the specific surface area of the packing and the mean film thickness:

$$h_L = a_p \delta \quad (7)$$

For purposes of hydraulic calculations, the film thickness can be calculated from the well known Nusselt falling film expression adapted for the inclined wall situation:

$$\delta = \left( \frac{3\mu_L u_{Ls}}{\rho_L g a_p \sin \alpha} \right)^{\frac{1}{3}} \quad (8)$$

where subscript  $L$  refers to the liquid, and  $g$  is gravitational acceleration.

With film thickness from equation (8), the hydraulic diameter of the characteristic triangular gas flow channel follows from:

$$d_{hG} = \frac{\frac{(bh - 2\delta s)^2}{bh}}{\left[ \left( \frac{bh - 2\delta s}{2h} \right)^2 + \left( \frac{bh - 2\delta s}{b} \right)^2 \right]^{0.5} + \frac{bh - 2\delta s}{2h}} \quad (9)$$

where  $b$ ,  $h$  and  $s$  respectively represent the corrugation base length, corrugation height and corrugation side length.

Correlations describing pressure losses due to gas/liquid and gas/gas interactions are given in the Appendix, to provide complete information on the present version of the Delft model for predicting the hydraulic performance of structured packings.

Figure 7 shows a comparison of predicted and measured values of pressure drop as a function of column diameter for a given liquid load. The agreement in the preloading region is nearly perfect, with the exception of the lowest diameter, which, however, can be improved significantly if one simulates the observed strong wall-wiper effect by a corresponding reduction in column diameter.

According to the model, the diameter effect practically ceases at column diameters above 1 m, which is in agreement with observations. However, the model does not account for the shift in loading point (capacity) due to the diameter reducing effect. Also it suggests a slight increase in the loading point pressure drop, and that is contrary to the effect observed. From this point of view, an extension of the present correlation is needed to account appropriately for the observed loading point shift, as well as for the intensity of pressure drop enhancement in the loading region.

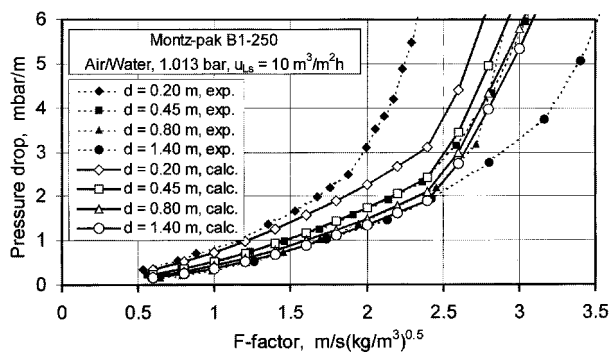


Figure 7. Predicted vs. measured pressure drop.

## CONCLUDING REMARKS

Although the absolute accuracy of the presented results is not as certain as it would be in the case of a series of experiments carried out using a single test installation, the trends are clear and indicative enough. The pressure drop of a corrugated sheet structured packing increases and, consequently, the packing capacity decreases with decreasing column diameter. This effect, limited to column diameters below 1 m, intensifies when the column diameter approaches the value equal to that of the height of a packing element, and it is more pronounced under wet than under dry conditions.

A practical consequence of this observation is that predictions based on academic scale data can lead to grave overestimates in the pressure drop and consequently column diameter, when applied to industrial scale columns.

Putting aside the possible contribution of a wall wiper, the increased pressure drop in small diameter columns can be attributed mainly to a relatively larger number of direction changes and related entrance effects enhanced by an increased liquid loading in the wall zone.

Because of the absence of any perforations in the surface of the packing used in this study, it may be expected that this study actually represents the worst case. The effect should diminish accordingly in the case of an increased corrugation angle, and/or a reduced packing element height, and/or enlargement in corrugation dimensions.

In the Delft model, the observed diameter effect is taken into account in the correlation describing the pressure loss due to flow direction changes, and the predictions are conservative enough for industrial scale columns. However, scale-down to small diameters is on the optimistic side, and the present loading point correlation has to be extended to account for the accompanying decrease in capacity.

## APPENDIX

In addition to the direction change imposed losses, the gas phase ascending through an irrigated bed consisting of corrugated sheet structured packing also experiences frictional pressure loss. One source is gas/liquid friction at the surface of the descending liquid film and the other more pronounced one is the interaction of gas flows at the interfaces created between crossing gas flow channels.

Overall gas/liquid interaction coefficient<sup>8</sup>:

$$\zeta_{GL} = \lambda \xi_{GL} \frac{h_{pb}}{d_{hG} \sin \alpha}$$

where  $\lambda$  represents the wetted perimeter of the triangular gas flow channel,  $\lambda = 2s/(b + 2s)$ , and  $\xi_{GL}$  is the friction factor. Friction between gas and liquid is approximated by an explicit form<sup>9</sup> of the well known Colebrook and White equation, where the absolute roughness of the surface is approximated by the film thickness:

$$\xi_{GL} = \left\{ -2 \log \left[ \frac{(\delta/d_{hG})}{3.7} - \frac{5.02}{Re_{Grv}} \log \left( \frac{(\delta/d_{hG})}{3.7} + \frac{14.5}{Re_{Grv}} \right) \right] \right\}^{-2}$$

$Re_{Grv}$  stands for a Reynolds number based on relative gas phase velocity:

$$Re_{Grv} = \frac{\rho_{Ge}(u_{Ge} + u_{Le})d_{hG}}{\mu_G}$$

with

$$u_{Le} = \frac{u_{Ls}}{a_p \delta}$$

as the mean film velocity.

Gas/gas interaction is related to the third, open side of the gas flow channel and it proved to be a strong function of corrugation inclination angle<sup>8</sup>:

$$\begin{aligned} \zeta_{GG} &= (1 - \lambda) \xi_{GG} \frac{h_{pb}}{d_{hG} \sin \alpha} \\ &= 0.722(1 - \lambda)(\cos \alpha)^{3.14} \frac{h_{pb}}{d_{hG} \sin \alpha} \end{aligned}$$

As indicated in equation (1) the change in the slope of the pressure drop in the loading regime is represented by an enhancement factor, which is applied when the gas load reaches the critical, loading point gas load.

Here the correlations for air/water system are given<sup>8</sup> as used in this study.

Loading point gas load:

$$F_{G,lp} = u_{Ge,lp}(\varepsilon - h_L) \sin \alpha \sqrt{\rho_G}$$

where the effective loading point gas velocity is described as

$$u_{Ge,lp} = \frac{(4294 u_{Ls} \cos \alpha) + 2.93}{(1453 u_{Ls} \cos \alpha) - \cos \alpha + 1.17} + \Omega$$

Pressure drop enhancement in the loading region:

$$F_{load} = 1453 u_{Ls} + \frac{1.17}{\cos \alpha} - \frac{4294 u_{Ls} + \frac{2.93}{\cos \alpha}}{u_{Ge} - \Omega}$$

Here,  $\Omega$  is a loading point constant which takes into account a shift in loading point due to openings in the surface of the packing. This is difficult to determine exactly, and for packings with holes it is assumed that this value is equal to the fraction of the surface occupied by holes. For Mellapak this would be 0.1, for Montz-pak BSH, 0.15 and for Montz-pak B1 it is certainly zero. For packings with slits forcing the gas to go to the other side of the sheet, for instance Ralu-pak and Gempak AW, this number could differ considerably.

## NOMENCLATURE

$a_p$	specific surface area of packing, $\text{m}^2 \text{m}^{-3}$
$b$	corrugation base length, m
$d_c$	column diameter, m
$d_{hG}$	hydraulic diameter for the gas phase, m
$F_{G,lp}$	loading point gas load factor, $\text{m s}^{-1} (\text{kg m}^{-3})^{0.5}$
$F_{load}$	loading effect factor, –
$g$	gravity acceleration, $\text{m s}^{-2}$
$h$	corrugation height, m
$h_L$	liquid hold up, –
$h_{pb}$	height of the packed bed, m
$h_{pe}$	height of the packing element, m
$Re_{Ge}$	effective gas phase Reynolds number, –
$Re_{Gr}$	relative velocity Reynolds number, –

$s$	corrugation side length, m
$u_{Ge}$	effective gas velocity, $\text{m s}^{-1}$
$u_{Ge,lp}$	effective loading point gas velocity, $\text{m s}^{-1}$
$u_{Gs}$	superficial gas velocity, $\text{m s}^{-1}$
$u_{Le}$	effective liquid velocity, $\text{m s}^{-1}$
$u_{Ls}$	superficial liquid velocity, $\text{m s}^{-1}$

## Greek letters

$\alpha$	corrugation inclination angle, °
$\delta$	liquid film thickness, m
$\varepsilon$	packing porosity, $\text{m}^3 \text{voids/m}^3 \text{bed}$
$\lambda$	fraction of the triangular flow channel occupied by liquid, –
$\mu_G$	viscosity of gas, Pa s
$\mu_L$	viscosity of liquid, Pa s
$\rho_G$	density of gas, $\text{kg m}^{-3}$
$\rho_L$	density of liquid, $\text{kg m}^{-3}$
$\zeta_{DC}$	overall coefficient for direction change losses, –
$\zeta_{GG}$	overall coefficient for gas-gas friction losses, –
$\zeta_{GL}$	overall coefficient for gas-liquid friction losses, –
$\xi_{bulk}$	direction change factor for bulk zone, –
$\xi_{GG}$	gas-gas friction factor, –
$\xi_{GL}$	gas-liquid friction factor, –
$\xi_{wall}$	direction change factor for wall zone, –
$\psi$	fraction of gas flow channels ending at column walls, –

## REFERENCES

1. Billet, R., 1989, *Packed Column Analysis and Design*, (Ruhr-University Bochum).
2. Meier, W., Hunkelar, R. and Stoecker, D., 1979, Performance of the new regular tower packing 'Mellapak', *ICHEME Symp Ser No. 56*: 2: 3.3/1–17.
3. McNulty, K. J. and Hsieh, C. L., 1982, Hydraulic performance and efficiency of Koch Flexipac structured packings, *AIChE Annual Meeting, Los Angeles, Nov. 14–19*.
4. Kister, H., 1992, *Distillation Design*, (McGraw-Hill, New York).
5. Brunazzi, E. and Paglianti, A., 1997, Mechanistic pressure drop model for columns containing structured packings, *AIChE J*, 43: 317–327.
6. Olujić, Z. and de Graauw, J., 1994, Effects of geometrical features on pressure drop of corrugated sheet structured packings, *AIChE Annual Meeting, San Francisco, Nov 13–18*. Paper 132f.
7. Stikkelman, R. de Graauw, J., Olujić, Z., Teeuw, H. and Wesselingh, H., 1989, A study of gas and liquid distributions in structured packings, *Chem Eng Tech*, 12: 445–449.
8. Olujić, Z., 1997, Development of a complete simulation model for predicting the hydraulic and separation performance of distillation columns equipped with structured packings, *Chem Biochem Eng Q*, 11: 31–46.
9. Olujić, Z., 1981, Compute friction factors fast for flow in pipes, *Chem Eng*, 88, (25): 91–93.

## ACKNOWLEDGEMENTS

The author gratefully acknowledges the continuous material support and co-operation of J. Montz GmbH in this study. He is also indebted to graduate students: H. Poelwijk, L. Voogd, J. M. Matthijsse, T. Bavelaar, M. Behrens and P. Saraber who have carried out and/or double checked measurements reported in this study.

## ADDRESS

Correspondence concerning this paper should be addressed to Z. Olujić, Laboratory for Process Equipment, TU Delft, Leehwaterstraat 44, 2628 CA Delft, The Netherlands. (E-mail: z.olujic@wbmt.tudelft.nl).

*The manuscript was received 1 February 1999 and accepted for publication after revision 3 June 1999. This paper was presented partly, as a poster, at the AIChE Annual Meeting, held in Miami Beach, 15–20 November, 1998.*